

# Update on the Development of High Performance Anti-Reflecting Surface Relief Micro-Structures

Douglas S. Hobbs\*, Bruce D. MacLeod, and Juanita R. Riccobono

TelAztec LLC, 15 A Street, Burlington, Massachusetts 01803 USA

## ABSTRACT

Microstructures built into the surfaces of an optic or window, have been shown to suppress the reflection of broad-band light to unprecedented levels. These antireflective (AR) microstructures form an integral part of an optic component, yielding an AR property that is as environmentally robust, mechanically durable, and as radiation-hardened as the bulk material. In addition, AR microstructures built into inexpensive glass windows, are shown below to exhibit a threshold for damage from high energy lasers of nearly  $60 \text{ J/cm}^2$ , a factor of 2 to 4 increase over published data for conventional thin-film dielectric material AR coatings.

Three types of AR surface relief microstructures are being developed for a wide variety of applications utilizing light within the visible to very long wave infrared spectrum. For applications requiring broad-band operation, Motheye AR textures consisting of a regular periodic array of cone or hole like structures, are preferred. Narrow-band applications such as laser communications, can utilize the very high performance afforded by sub-wavelength structure, or SWS AR textures that consist of a periodic array of simple binary, or step profile structures. Lastly, Random AR textures offer very broad-band performance with a simple manufacturing process, a combination that proves useful for cost sensitive applications such as solar cells, and for complex devices such as silicon and HgCdTe sensor arrays.

An update on the development of AR microstructures is discussed for many specific applications. Data from SEM analysis, reflection and transmission measurements, environmental durability testing, and laser damage testing, is shown for AR microstructures fabricated in silicon, fused silica, borofloat glass, ZnGeP, AMTIR, As<sub>2</sub>Se<sub>3</sub>, As<sub>2</sub>S<sub>3</sub>, and GaAs.

**Keywords:** Anti-Reflection, Motheye, Microstructures, Radiation-Hardened, Laser Damage Threshold, Coatings

## 1. INTRODUCTION

Light reflected from windows, lasing crystals, and optics within many high-power laser systems can cause the failure of laser components such as the pump diodes, limiting the lifetime and the amount of laser energy that can be extracted. This in turn limits the range of laser communications systems and laser environmental sensors, and reduces the amount of laser energy delivered in medical lasers, laser weapons, and laser fusion systems<sup>[1-6]</sup>. Imaging systems such as visible-light cameras and infrared focal plane arrays, have a vulnerability to reflected light from internal windows, imaging optics, and in particular the highly reflective surface of the detector array. These stray light reflections cause ghost images and increased background noise that both serve to reduce the sensor's effectiveness, and in the case of silicon detectors, the quantum efficiency of the detector is critically dependent on the elimination of reflected light<sup>[7]</sup>. In a related manner, the efficiency of solar cells could be dramatically improved if a cost effective means for suppressing light reflections could be developed that operates over a broader spectral range and most significantly over a wide incident angle range<sup>[8]</sup>.

Suppressing reflections from optics and windows has long been accomplished by depositing multiple thin layers of dielectric materials onto each external surface of the window or optic. Each deposited layer of material is designed to affect constructive or destructive interference for a given wavelength propagating through the window or optic surface. Because of the necessary interference effect, the optical field amplitude present at each material layer interface is large, leading to thermal gradients and rapid damage near coating defects for relatively low optical energy. For broad-band anti-reflection (AR) coatings, a great number of thin-film layers are needed. With visible or infrared imaging systems,

---

\* Correspondence: [DSHobbs@telaztec.com](mailto:DSHobbs@telaztec.com), Voice: 781-229-9905, Fax: 781-229-2195 [www.telaztec.com](http://www.telaztec.com)

multiple layer thin-film coating stacks can produce an increase in reflected light and undesirable polarization effects for high angle (stray) light incident off the system axis.

Thin-film AR coatings are limited to applications where;

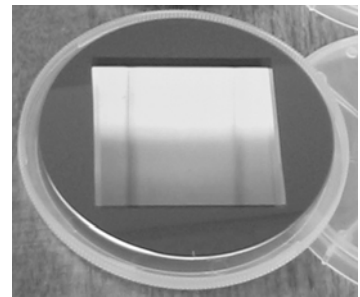
- 1) The optical fluence is low (e.g.  $< 20\text{J}/\text{cm}^2$  at 1064nm for fused silica optics), and/or;
- 2) The radiation level is low (e.g.  $< 300\text{KRad}$  Si proton exposure), and/or;
- 3) The environmental variations are low (temperature and humidity), and/or;
- 4) The environment is not abrasive (rain and sand erosion), and/or;
- 5) The bandwidth is limited to  $< 1$  octave (e.g. 400-700nm, 800-1100nm, 1.5-1.6 $\mu\text{m}$ , 3-5  $\mu\text{m}$ , 8-12 $\mu\text{m}$ ), and/or;
- 6) The light incident angle range is less than 30 degrees, and/or;
- 7) The cost of the AR coating is not the primary concern.

For all of these application areas, the development of an AR treatment based on surface relief microstructures built directly in the window or optic material, can provide breakthrough performance, reduced cost, and increased lifetime particularly in the harsh environments of space and the abrasive environments typical of military operations.

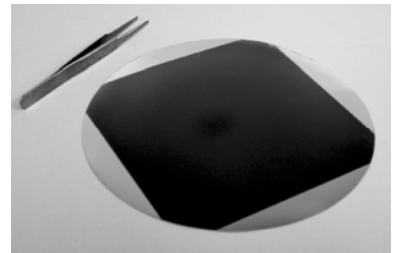
## 2. MICROSTRUCTURE BASED ANTI-REFLECTION TECHNOLOGY

When the typically smooth external surface of an optic or window is roughened to produce a dense texture consisting of surface relief microstructures with a height and spacing that is small compared to the wavelength of light to be employed, light propagating through the texture will encounter a gradual change of the refractive index as it enters the bulk optic material. With a sufficiently gradual change, there will be no reflected light. Such an effect is commonly known as the Motheye principle<sup>[9-12]</sup>, due to the observation that cone-like protruberances on the eyes of night flying moths serve to suppress visible light reflections making the moth less visible to owls. The design, fabrication, and AR performance of Motheye structures has been previously described for a variety of materials and applications<sup>[8,13-15]</sup> where durability, radiation resistance, cost, viewing angle, or broad-band performance are critical.

To fabricate periodic Motheye AR structures in any material surface, the process begins with an initial patterning or lithography step<sup>[15-16]</sup>. The Motheye pattern is recorded in a sacrificial light sensitive material that is in turn used as a mask in a dry etching process designed to transfer the mask pattern into the surface of the window or optic material. Motheye AR textures typically consist of regular arrays of cone, hole, or post structures, repeated on a square or honeycomb grid. A four-inch diameter gallium arsenide (GaAs) window etched with Motheye AR textures designed to suppress mid-IR light reflections is shown on the right. The central square region contains an array of cone structures with a 520nm spacing. For some applications requiring broad-band stealth, diffraction from the periodic Motheye texture of light with wavelengths less than the design range, can be undesirable. Visible light diffraction from Motheye structures designed for near infrared or MWIR performance, is typically quite noticeable - as indicated by the bright (blue-green) diffracted light in the image above. To eliminate this diffraction, TelAztec has developed (patent pending) a process and design for AR textures that have a random distribution of sub-wavelength-sized surface features. The random distribution prevents the short wavelength reflected light from adding constructively in any direction.



Perhaps the largest benefit of random AR textures is a greatly simplified fabrication process that does not require lithography. As described below, random AR textures designed for operation in the visible and near infrared regions have been produced in materials such as Schott borofloat glass, fused silica, zinc germanium phosphide (ZGP), silicon, cadmium zinc telluride (CZT), and several types of plastic. Windows or lenses as large as 12-inch in diameter can be realized in the short term, with 8-inch diameter windows currently being converted into hard nickel injection molding tools like that shown in the photograph on the right. Such a hard metal master may also prove useful for molding AR microstructures into infrared glasses such as AMTIR, BGG, As<sub>2</sub>S<sub>3</sub> and As<sub>2</sub>Se<sub>3</sub>. Plastic materials have a particular advantage in that they can be fabricated using high volume replication methods.



Scanning Electron Microscope (SEM) photographs of a Random texture AR microstructure etched into the surface of glass, is shown below in Figure 1. The size of the majority of the structures in this carpet-like texture is much less than the visible to NIR wavelengths that will pass through the window. Extremely broad-band AR performance is found with these structures as show in Figure 2. Data for the reflectance from the Random texture AR treatment was recorded by Janos Technologies using their Perkin Elmer FTIR. Reflectance levels of less than two-tenths of one percent (0.2%) from 400nm to 1100nm are found, with no more than 0.4% over the range from 400nm to 2000nm in prototype #Plano6. Note the extremely low levels recorded at the communications wavelength bands at 1310 and 1550nm (more detailed data covering this band is given below). There are laser communications and high-power laser applications that would gain an immediate benefit from such a high performance AR treatment.

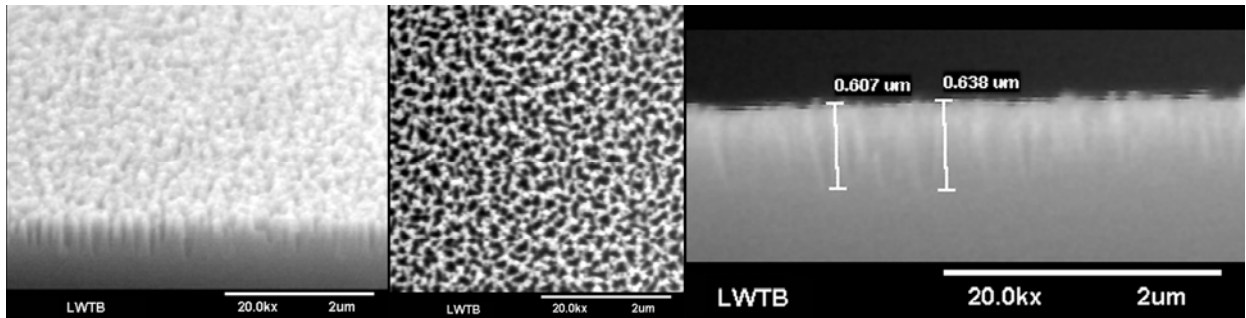


Figure 1: SEM images showing elevation, overhead, and profile views of Random AR textures fabricated in a glass window.

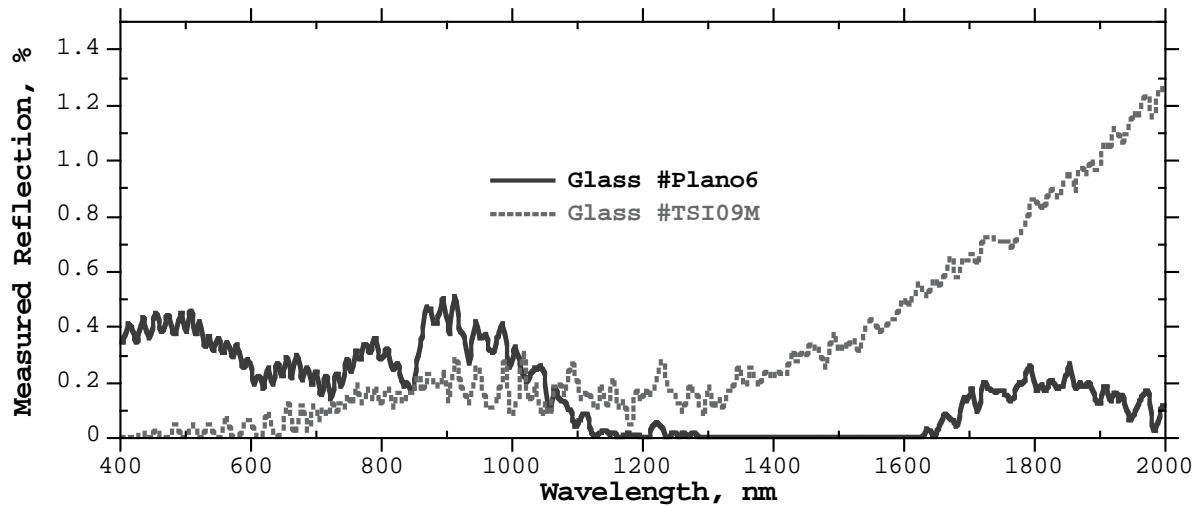


Figure 2: Measured reflectance of visible/NIR light from Random AR textures fabricated in a glass window.

### 3. PERFORMANCE MEASUREMENTS

To determine the AR performance of the fabricated surface relief microstructures, both transmission and reflection measurements are made using a grating-based, fiber-coupled white light spectrometer for prototypes designed to operate on visible to near infrared (NIR) light (400-1000nm), an Agilent Optical Spectrum Analyzer for precision reflection measurements of AR structures intended for operation in the NIR around 1550nm, and a Nicolet FTIR spectrometer for transmission measurements of AR structures designed for infrared operation over the range of from 1.8 to 16 µm. The profile and sizes of the AR structures are also characterized by scanning electron microscope (SEM) analysis.

Data collected for a variety of AR microstructures fabricated in various materials of interest for applications covering the visible through the infrared spectrum, is given below. The data is presented in order of the spectral range targeted, with the shorter wavelength designs presented first.

### 3.1 VISIBLE – NIR, 400-2000nm: MATERIALS / APPLICATIONS

Throughout the visible spectral region there are mainly applications for glass and plastic materials that require a high performance AR treatment that can be produced at low cost. These applications include display covers, eyeglasses and windows, rifle, periscope, and telescope optics, and digital camera lenses. Secondary to cost, these applications require an AR treatment that is environmentally robust and one that can be repeatedly cleaned. AR microstructures that are molded or replicated in scratch resistant plastics offer a very low cost solution.

Applications involving AR treatments for visible light detectors based on silicon can support higher costs but require very high AR performance where the AR microstructure fabrication must be integrated with the sensor manufacturing process. In a related manner, silicon-based solar cells incorporating AR microstructures may yield a significantly increased efficiency leading to smaller panels producing more electricity without the need to track the movement of the sun. Both thin and thick film solar cells could benefit from the integration of AR microstructures if a low cost fabrication process can be developed.

#### 3.1.1 Borosilicate Glass, Schott Borofloat 33, (n = 1.48)

A process for fabricating random distribution AR microstructures directly in the surface of inexpensive borosilicate glass has been developed. Typical AR performance of the micro-textured glass is shown in Figure 2 above. One application of this glass is for protective covers over earth-based solar panels. To evaluate the environmental durability of the micro-textured glass for the solar panel application, a 3-inch diameter window prototype was subjected to a 24-hour variable humidity and temperature test using a Tenney Environmental Test chamber. Omega Optical, Inc., a prominent optical filter manufacturer based in Vermont, conducted the tests using their facility and following the Natural Environment Procedure outlined in Method 507.3 of military standard Mil-Std-810E. The results are shown in Figure 3. The dashed black curve shows the transmission of the window at the start of the tests. Note the greater than 99% transmission from 500 to 2000nm (relative to a typical 92.5% transmission for untreated glass). The solid grey line shows the transmission of the window after 10 days of exposure, where the transmission has decreased by less than 0.3%. Another approximately 0.3% decrease is seen only at wavelengths less than 900nm after 30 days of exposure (solid black curve). After each measurement, the window was cleaned using a simple solvent rinse followed by air drying and a repeat of the measurement. No transmission changes were observed after repeated cleaning cycles. The tests are an initial indication that the fine AR microstructures may be durable enough for the solar panel application.

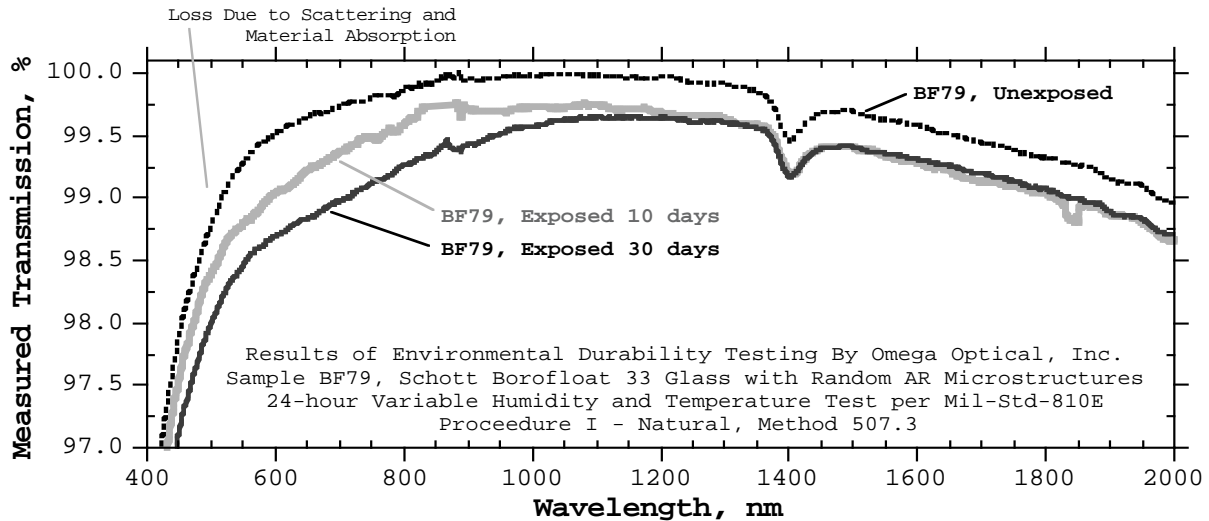


Figure 3: Measured transmission of a glass window with random AR textures fabricated in both surfaces. The transmission was measured before and after 10 and 30 day exposures to varied temperature and humidity conditions.

Because of the graded index nature of AR microstructure technology, it is expected that a window or optic incorporating AR surface relief microstructures will pass a greater amount of optical energy without damage than conventional thin-film coatings. An initial test of this concept was performed using Random AR microstructures etched into both external surfaces of an 80mm diameter, 2.75mm thick Schott Borofloat 33 glass window identified as sample BF91. A laser damage test was first performed by Schott North America of Pennsylvania using a 1064nm laser with an 8ns pulse

length and a fluence of  $\geq 6 \text{ J/cm}^2$ . This is a standard test that Schott performs as a quality control. A grid of about 10 locations on the window were exposed to 5 pulses. None of the areas showed any damage. Next the same part was sent to Big Sky Laser, Inc. in Montana to perform a more thorough test aimed at finding the laser damage threshold. Big Sky exposed more than 100 locations to 10 different fluence levels using a 1064nm pulsed laser with a 20ns pulse length and a 0.5mm spot size ( $1/e^2$ ). The pulse repetition rate was 20Hz allowing 200 pulses at each location (10 sec dwell time). The criteria for damage was a permanent surface change as observed by visual inspection through a microscope. The test was repeated for a second sample of Schott glass with no AR treatment. Both glass samples were cleaned prior to the test with a standard acid ( $\text{H}_2\text{SO}_4:\text{H}_2\text{O}_2$ ) immersion and solvent rinse followed by a nitrogen blow dry. The results are shown in Figure 4 where the damage threshold for the glass with the AR microstructures is  $56.8 \text{ J/cm}^2$ , and the damage threshold for the untreated window is  $38.3 \text{ J/cm}^2$ . To our knowledge, the nearly  $60 \text{ J/cm}^2$  damage threshold of AR microstructures in glass is about 3 times greater than the best published data for single-layer thin-film coatings on fused silica<sup>[2-5]</sup>. A repeat of the test is planned using other types of AR microstructures and other glasses such as Schott BK7 and fused silica.

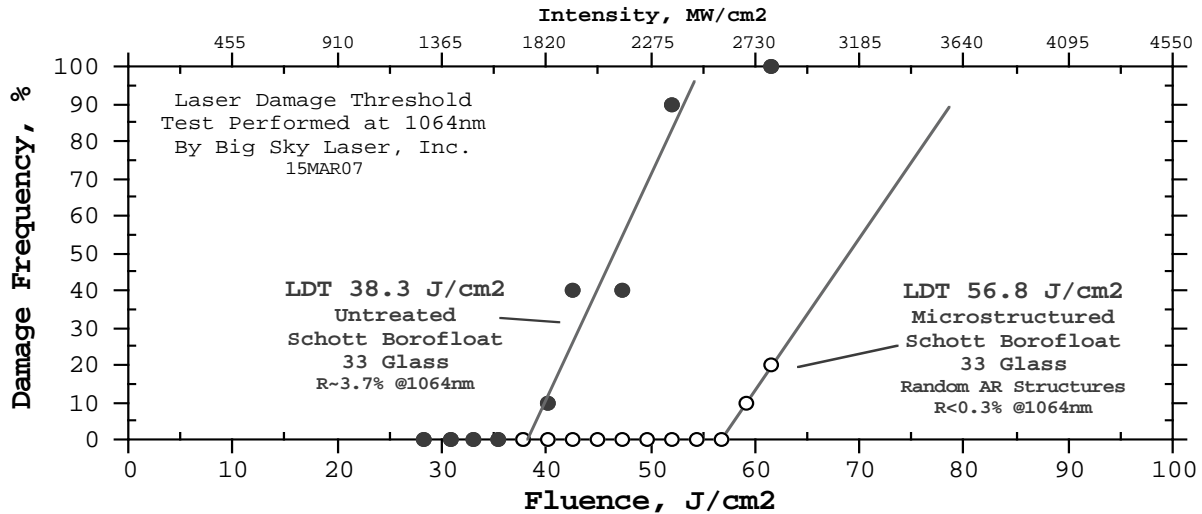


Figure 4: Results of a laser damage threshold on Schott glass windows with and without AR microstructures.

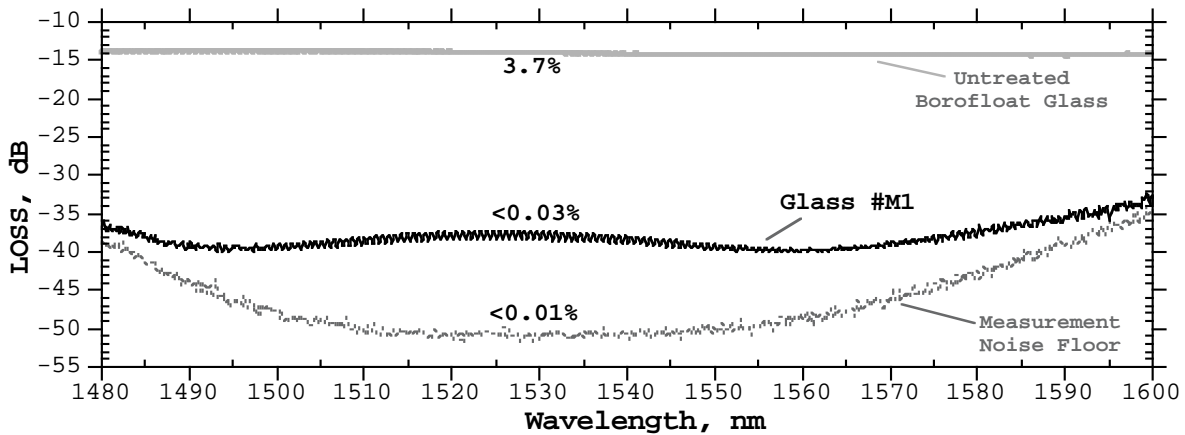


Figure 5: Measured reflection of NIR light from Random AR microstructures in a Schott borofloat glass window.

As noted above in Figure 2, exceptional AR performance is achieved with Random AR microstructures over the NIR wavelengths used with fiber optic telecommunications systems. A more accurate measurement of the reflection from a Random AR texture fabricated in Schott Borofloat glass was performed using an Agilent Optical Spectrum Analyzer (OSA) and a fiber coupled LED light source. Figure 5 shows the reflection loss plotted on a log scale over the wavelength range of from 1480 to 1600nm. The OSA noise floor (measured signal with a covered probe) is plotted

showing that measurements down to 0.01% are possible. For reference the measured reflection of an untreated borofloat window is shown at the top of the plot (~3.7%). Sample M1 shows a reflection loss below -35dB (<0.03%) over the entire telecommunications C and L bands.

### 3.1.2 Fused Silica, SiO<sub>2</sub>, (n = 1.46)

Fused silica is a high purity glass that sees extensive use in high power laser systems and in telecommunications. A process for fabricating Random texture AR structures in fused silica is under development. To date the best AR performance obtained is shown in Figure 7 where the visible light reflection is less than 0.5% rising to just over 1% at 1000nm in the NIR. The fabricated structure is shown in Figure 6. With further optimization of the structure profile, the broad-band AR performance found with Random textures in borofloat glass should be obtained.

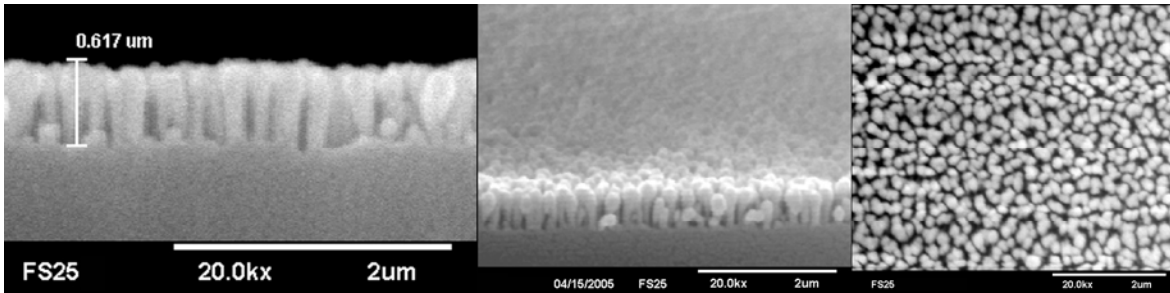


Figure 6: SEM photographs of Random AR textures fabricated in a fused silica window.

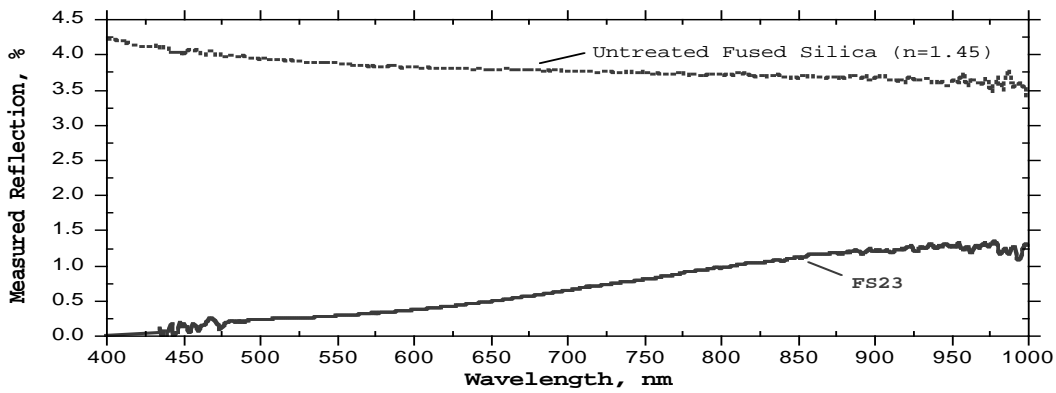


Figure 7: Measured reflection of Random AR textures fabricated in a fused silica window.

### 3.1.3 PLASTIC: Polycarbonate, Polyethylene, Cast Acrylic, (n = 1.49 to 1.61)

The Random AR textures shown in Figures 1 and 6 have been replicated into plastic using a variety of methods such as casting into UV-curable acrylics, and direct embossing. Figure 8 shows a typical casting of a Random AR texture in a scratch resistant plastic intended for application as automotive instrument panel covers, ultra-black textures for synthetic clothing and automotive dashboards, and display covers for portable devices. Figure 9 shows an image of an automobile instrument panel mock up where one half of the plastic cover has been replaced by a Random AR textured window. Note that the reflection from a typical office light fixture completely obscures the instruments behind the untreated window, whereas the treated window shows the instruments clearly.

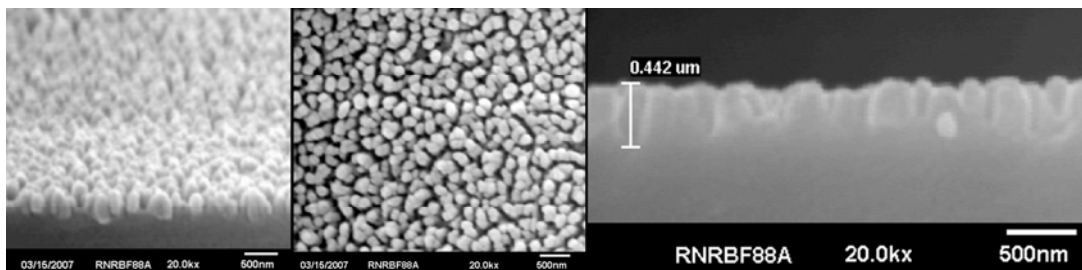


Figure 8: SEM photographs of Random AR textures replicated in a plastic window.

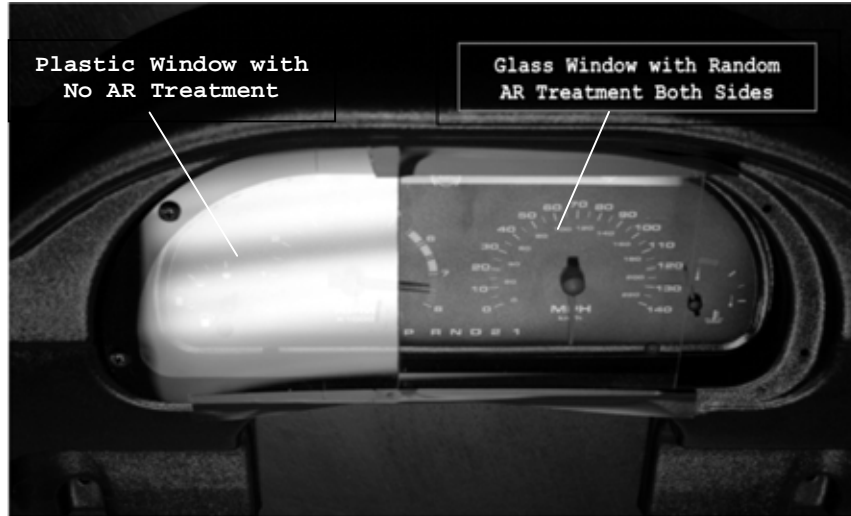


Figure 9: Instrument panel mockup showing reflections from untreated (left) and treated (right) covers.

### 3.1.4 Silicon, Si, ( $n = 3.42$ )

The imaging sensors in typical digital cameras convert light into an electrical signal using silicon semiconductor technology. Visible light is absorbed at the sensor surface that is composed of the highly reflective and common material silicon. Without an AR treatment, silicon will reflect more than 35% of visible light. This represents an unacceptable loss for silicon-based cameras, and a severe degradation in the efficiency of related silicon solar cells. AR microstructures have been designed and fabricated in silicon windows for imaging sensor and solar cell applications. Both Random AR textures like that shown in Figure 10, and Motheye AR textures like that shown in Figure 11 have been produced. The AR performance of these textures is exceptional as shown in Figure 12, where for the Motheye textures the reflection has been reduced from over 35% down to less than 0.5% over the entire visible-NIR range.

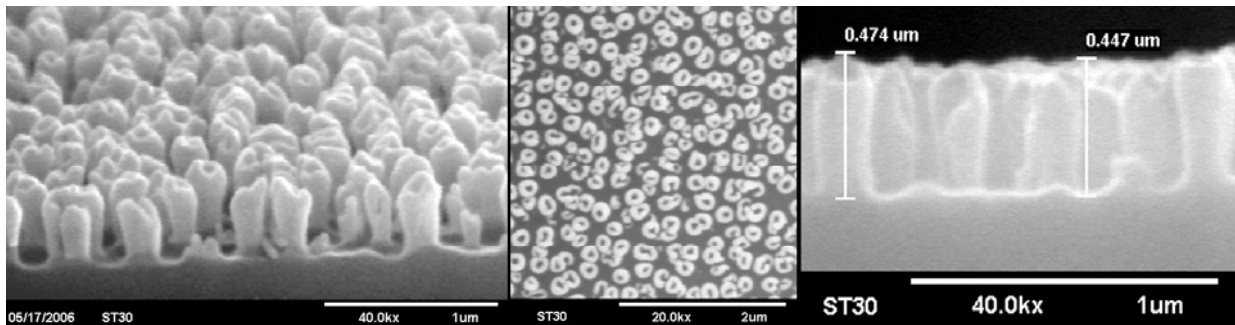


Figure 10: SEM photographs of Random AR textures designed for the visible fabricated in a silicon window.

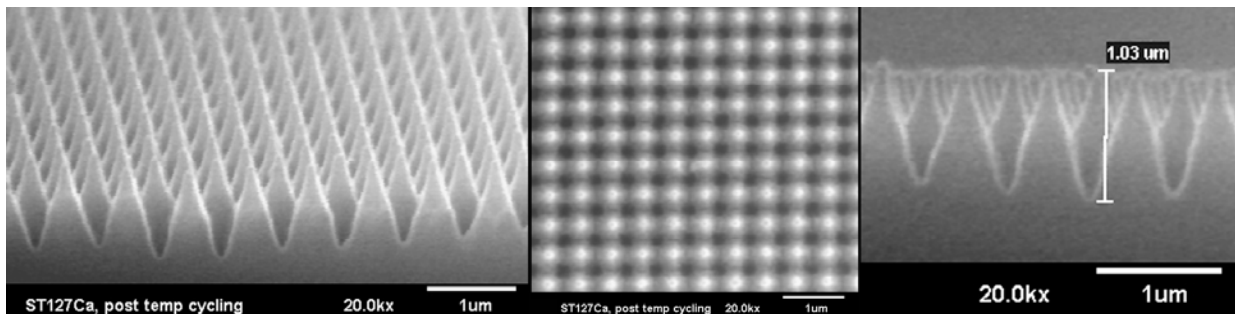


Figure 11: SEM photographs of Motheye AR textures designed for the visible/NIR fabricated in a silicon window.

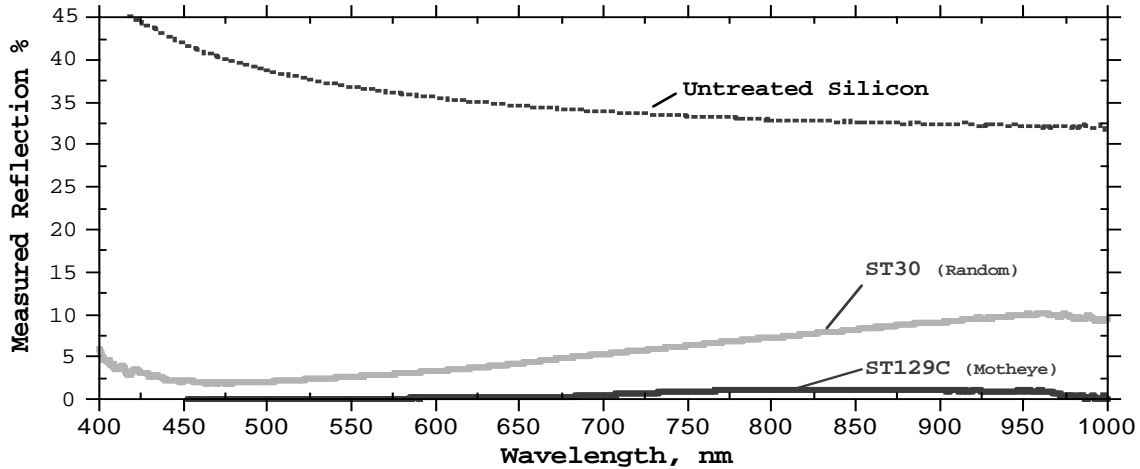


Figure 12: Measured reflection of silicon windows incorporating Motheye (ST129C) and Random (ST30) AR textures.

### 3.2 Mid-IR, 2-5 $\mu\text{m}$ : MATERIALS / APPLICATIONS

The mid-IR spectral band covering the wavelength range of from 2 to 5 microns, is important for military and commercial applications due to the low optical attenuation of the earth's atmosphere, and because gases and vapors have fundamental absorption lines in this wavelength range. Materials of interest in this wavelength region include GaAs used for sensor windows, zinc germanium phosphide (ZGP) crystals used to generate mid-IR light, and several chalcogenide glasses such as AMTIR,  $\text{As}_2\text{S}_3$ , and  $\text{As}_2\text{Se}_3$  used for inexpensive optics, fiber optics, and potentially moldable IR transmitting optics.

#### 3.2.1 Arsenic Tri-Sulfide, $\text{As}_2\text{S}_3$ , ( $n \sim 2.4$ )

Motheye AR textures were designed and fabricated in one surface of several one-inch diameter  $\text{As}_2\text{S}_3$  windows supplied by the Naval Research Labs.  $\text{As}_2\text{S}_3$  windows have a refractive index of about 2.4 and appear dark red. The structures were patterned in a mask layer using interference lithography and then transferred into the material surface using ion milling. Figure 13 shows the pyramidal type structures fabricated where the structure spacing is 700nm and the structure height is about 1200nm. Figure 14 shows the transmission of the Motheye textured window (solid black curve) compared to the transmission of the untreated window (dashed black curve). (Note that the data within spectral regions containing  $\text{CO}_2$  and water vapor lines has been interpolated). An estimate of the maximum transmission attainable with no reflections from one surface is shown as the solid grey line. This estimate is based on the refractive index information provided by NRL. The data shows a transmission increase between 9 and 10% over the entire 2 to 5 micron target range. Further refinement of the process will involve larger structure spacing and deeper structures. An attempt to directly emboss such structures into the  $\text{As}_2\text{S}_3$  surface using a hard metal master mold is planned.

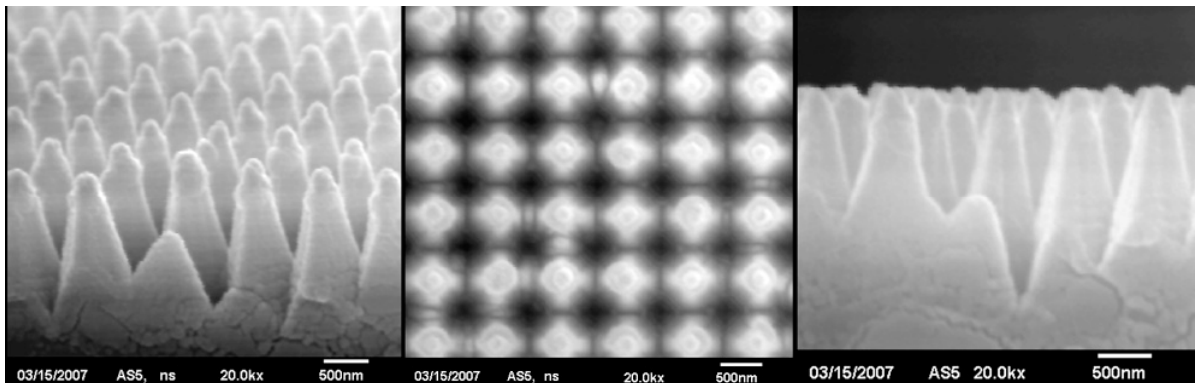


Figure 13: SEM photographs of AR microstructures fabricated in an  $\text{As}_2\text{S}_3$  window.



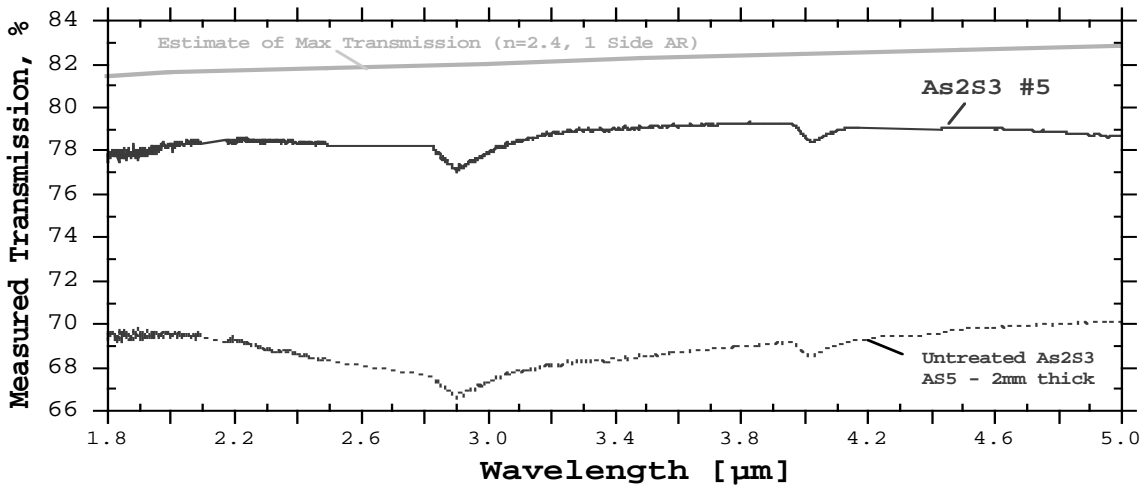


Figure 14: Measured transmission through an  $As_2S_3$  window with a Motheye AR texture fabricated in one surface only.

### 3.2.2 Arsenic Tri-Selenide, $As_2Se_3$ , ( $n \sim 2.76$ )

Motheye AR textures were designed and fabricated in one surface of several one-inch diameter  $As_2Se_3$  windows supplied by the Naval Research Labs.  $As_2Se_3$  windows have a refractive index of about 2.76 and have a dark grey appearance that is similar to AMTIR. The structures were patterned in a mask layer using interference lithography and then transferred into the material surface using ion milling. Figure 15 shows the pyramidal type structures fabricated in two different samples where the structure spacing is 600nm (top) and 700nm (bottom) and the structure height is over 900nm (top) and over 1200nm (bottom). Figure 16 shows the transmission of the Motheye textured windows compared to the transmission of an untreated window. An estimate of the maximum transmission attainable with no reflections from one surface is shown as the solid grey line at 78% (based on the refractive index information provided by NRL). Note that the differences between both the structure profile and structure depth for the two samples has a significant impact on the window transmission. Additional work is planned to determine the structure tradeoffs that arise when developing a molding process.

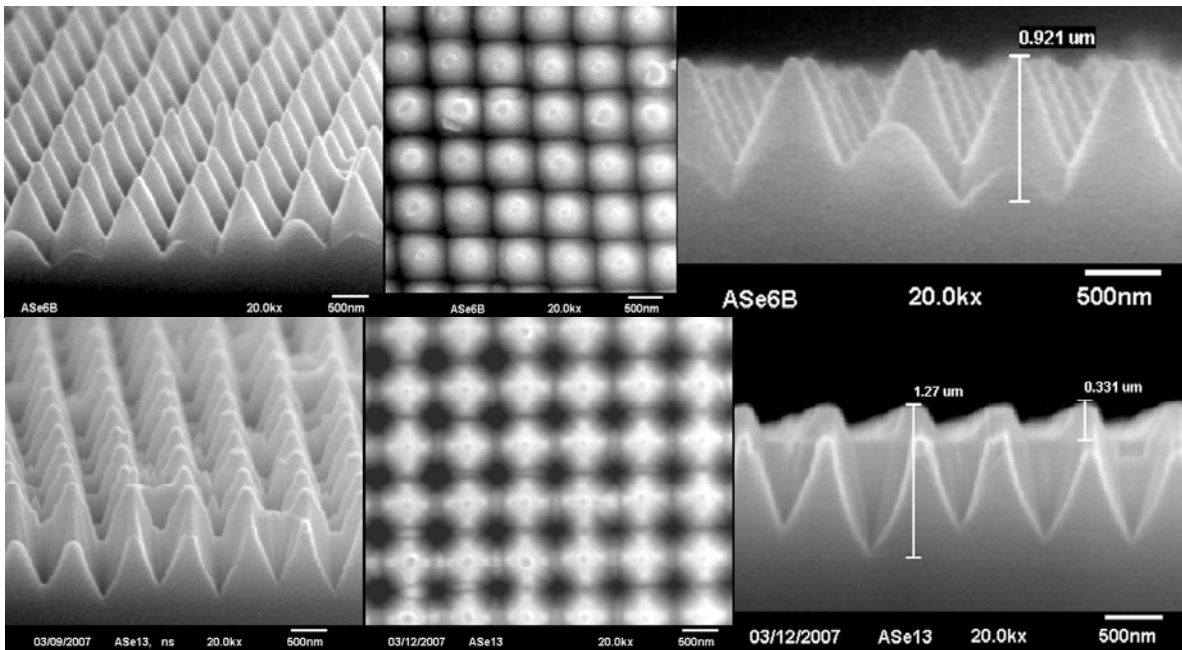


Figure 15: SEM photographs of AR textures fabricated in  $As_2Se_3$  windows.

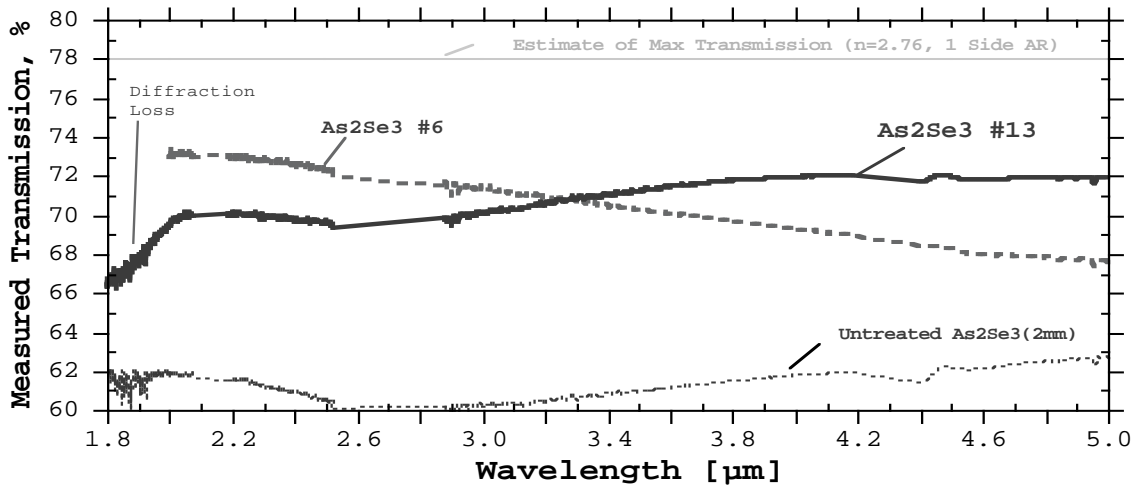


Figure 16: Measured transmission through As<sub>2</sub>Se<sub>3</sub> windows with a Motheye AR texture fabricated in one surface only.

### 3.2.3 Amorphous Material Transmitting IR, AMTIR, Ge<sub>33</sub>As<sub>12</sub>Se<sub>55</sub> (n = 2.5)

AMTIR is an amorphous glass-like material with a transmission range of from 750nm to 14 $\mu\text{m}$ . With a higher refractive index than ZnSe, AMTIR is a good choice for construction of lenses operating in both the MWIR and LWIR regions – two-color imaging applications. Motheye AR textures were fabricated into one surface of an AMTIR4 window supplied by Janos Technologies. Both MWIR and LWIR structures were produced. The results of this preliminary effort are shown in Figure 17. SEM images of the AR texture fabricated show the feasibility of fabricating high performance AR surfaces. Work to obtain transmission data for Motheye textured AMTIR windows is ongoing.

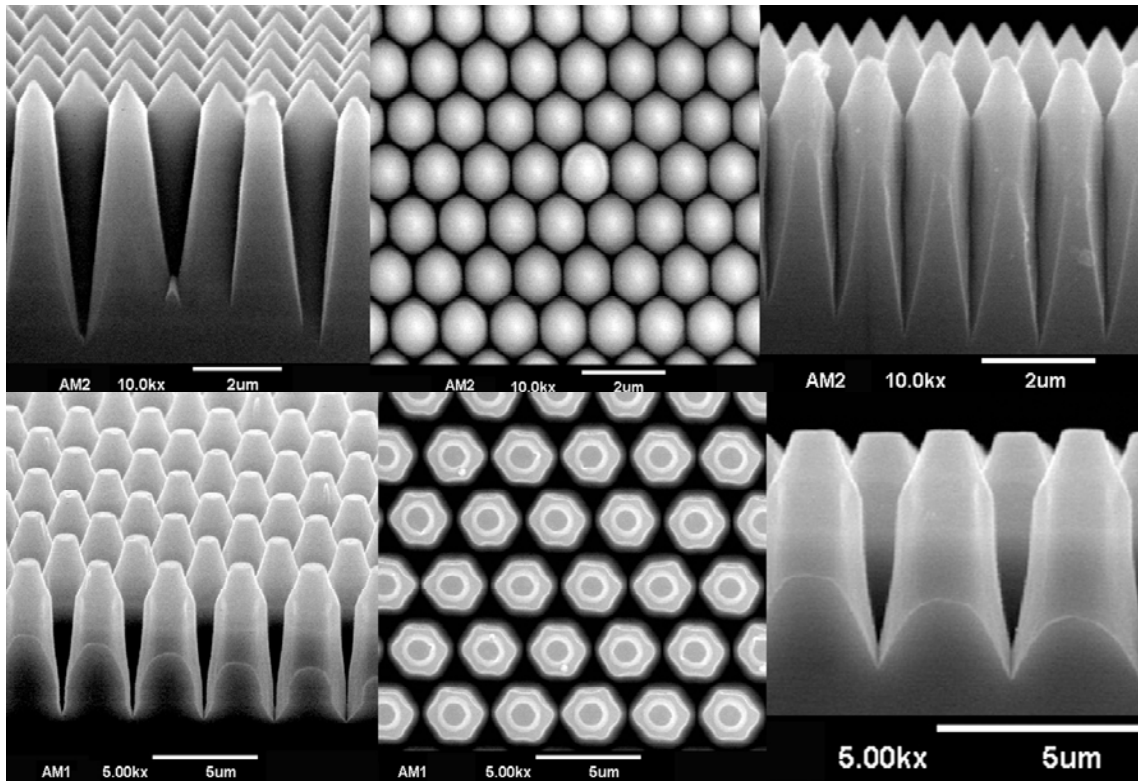


Figure 17: SEM images of AR textures etched in AMTIR4 windows designed for MWIR (top) and LWIR (bot) operation.

### 3.2.4 Gallium Arsenide, GaAs, (n = 3.3)

GaAs is a medium cost semiconductor material that has low absorption over the infrared range from 2 to 10 micron, making it useful as an optical window for various sensor systems. Motheye AR textures were designed and fabricated in GaAs windows as part of an ongoing project directed by MilSys Technologies of Pennsylvania. The structures were patterned in a mask layer using interference lithography and then transferred into the material surface using both reactive ion etching and ion milling processes. The goal was to fabricate high aspect ratio structures which would provide AR performance over a 10 micron bandwidth. Such deep pyramidal structures proved difficult to attain due mainly to the formation of etch blocking polymers during the pattern transfer process.

Figure 18 shows the best profile microstructures obtained using ion milling. Structure pitch is 520nm with a structure depth of about 750nm, just over 60% of the depth required for broad-band performance. The structure profile is tapered in a non linear fashion which enhances the performance, and the structure peaks are flat for better durability in abrasive environments. Figure 19 shows the transmission of the Motheye textured window over the mid-IR range. Peak performance is seen at 2.2 micron where the transmission has been increased from about 56% to 70%. The maximum transmission of 71% is also plotted in the figure as the grey line.

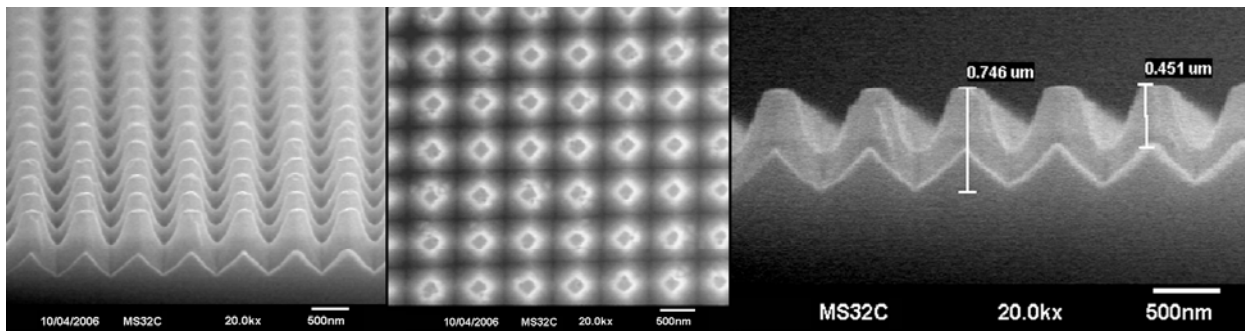


Figure 18: SEM photographs of AR textures fabricated in a GaAs window.

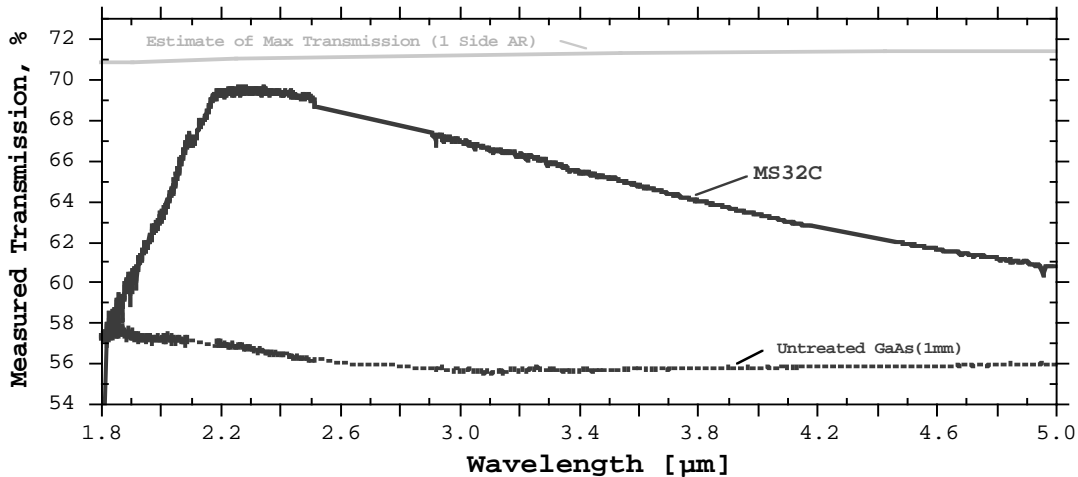


Figure 19: Measured transmission through a GaAs window with a Motheye AR texture fabricated in one surface only.

### 3.2.5 Zinc Germanium Phosphide, ZnGeP, (n = 3.13)

Laser sources operating at mid-IR wavelengths with moderate to high power output are primarily constructed as optical parametric oscillators (OPOs), where zinc germanium phosphide (ZnGeP<sub>2</sub> or ZGP) is the most common choice for the non-linear optical (NLO) lasing crystal used to generate mid-IR light from within the OPO<sup>[1]</sup>. ZGP OPOs are longitudinally pumped with 2.05 μm light and generate tunable MWIR light in the range of from 3.6 to 4.6 μm. The output power of ZGP-based OPOs has been limited by the low laser damage threshold of ZGP crystals employing thin-film AR coatings. AR microstructures are expected to make a significant improvement. In an SBIR Phase I project

sponsored by the Air Force Research Laboratory Materials and Manufacturing Directorate (WPAFB), AR microstructures were fabricated in ZGP windows supplied by BAE Systems of New Hampshire. The goal was to develop an AR microstructure fabrication process that could be used to generate broad-band AR performance on both faces of a ZGP crystal, and then to determine the laser damage threshold of the textured crystal. Both Random AR and Motheye AR structures were built using ion milling and reactive ion etching techniques. Figure 20 shows a typical Random AR texture, and Figure 21 shows the best performing Motheye AR structures fabricated to date. Figure 21 is a plot of the measured transmission through 6mm x 6mm x 2mm thick ZGP windows incorporating Random (#17) and Motheye (#41) AR microstructures. Both types of structures perform well at the pump wavelength of 2.05  $\mu\text{m}$ , but exhibit decreasing transmission over the signal and idler wavelength range from 3.5 to 4.5  $\mu\text{m}$ . Further work is needed to improve the MWIR transmission and to realize an AR microstructure fabrication process that can be used to generate textures on both faces of a 6mm x 6mm x 20mm ZGP crystal suitable for laser damage testing.

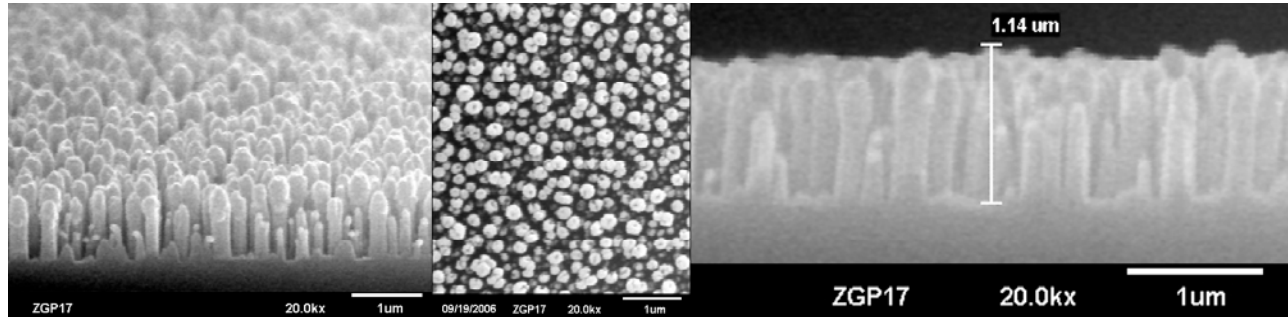


Figure 20: SEM photographs of Random AR textures designed for the mid-IR fabricated in a ZGP window.

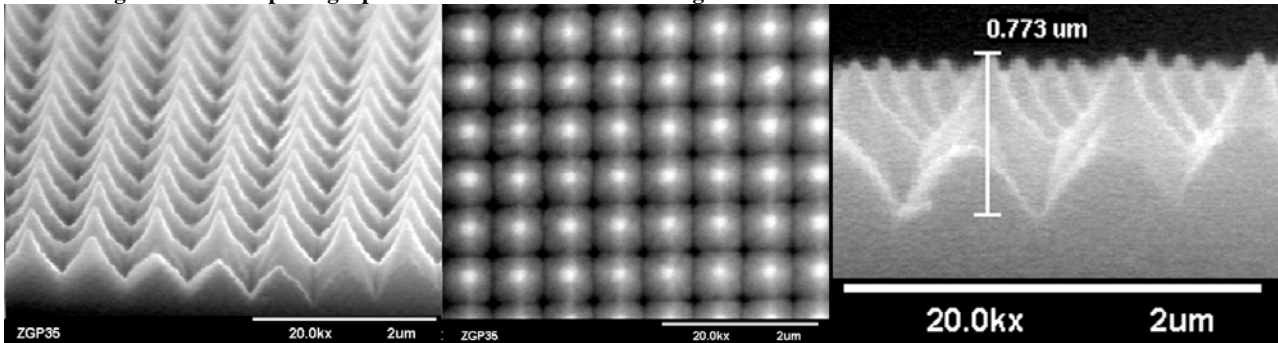


Figure 21: SEM photographs of Motheye AR textures designed for the mid-IR fabricated in a ZGP window.

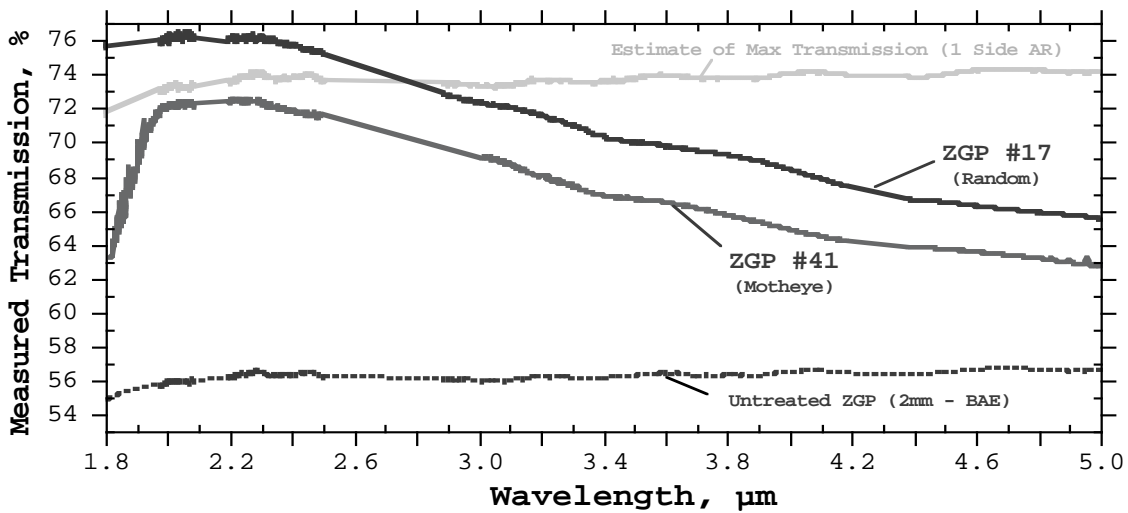


Figure 22: Measured transmission through ZGP windows with Random AR and Motheye textures fabricated in one surface.

### 3.3 Long-Wave-IR, 7-14 $\mu\text{m}$ : MATERIALS / APPLICATIONS

The LWIR spectral range is most useful for night vision sensors and industrial lasers. Motheye AR structures built in ZnSe, ZnS, Ge, and CdZnTe have been previously described<sup>[15]</sup>. Very few materials that transmit in this spectral region offer the potential for low cost moldable optics. One candidate material is  $\text{As}_2\text{Se}_3$  where the material can be drawn into fibers or molded into lenses. By creating high performance AR structures that can be molded simultaneously with the window or optic,  $\text{As}_2\text{Se}_3$  may benefit many LWIR applications.

#### 3.3.1 Arsenic Tri-Selenide, $\text{As}_2\text{Se}_3$ , ( $n \sim 2.76$ )

Motheye AR textures designed for LWIR operation, were fabricated in one surface of several one-inch diameter  $\text{As}_2\text{Se}_3$  windows supplied by the Naval Research Labs. Again, the structures were patterned in a mask layer using interference lithography and then transferred into the material surface using ion milling. Figure 23 shows the pyramidal type structures fabricated where the structure spacing is 2400nm and the structure height is over 3500nm. Figure 24 shows the transmission of the Motheye textured windows compared to the transmission of an untreated window. An estimate of the maximum transmission attainable with no reflections from one surface is shown as the solid grey line. The AR texture window shows a transmission increase of over 11% above the transmission measured for a window with no AR treatment, over the broad wavelength range of from 7 to 14 micron. Further refinements to the process can yield even higher broad-band transmission.

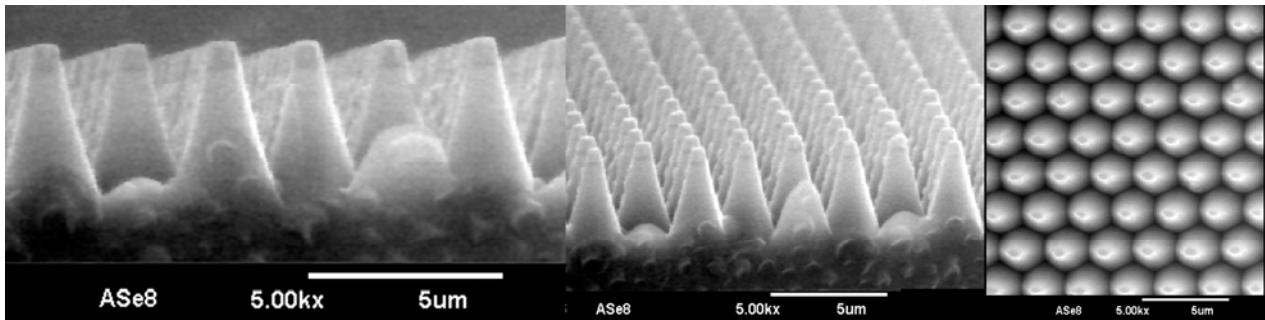


Figure 23: SEM photographs of AR textures fabricated in an  $\text{As}_2\text{Se}_3$  window.

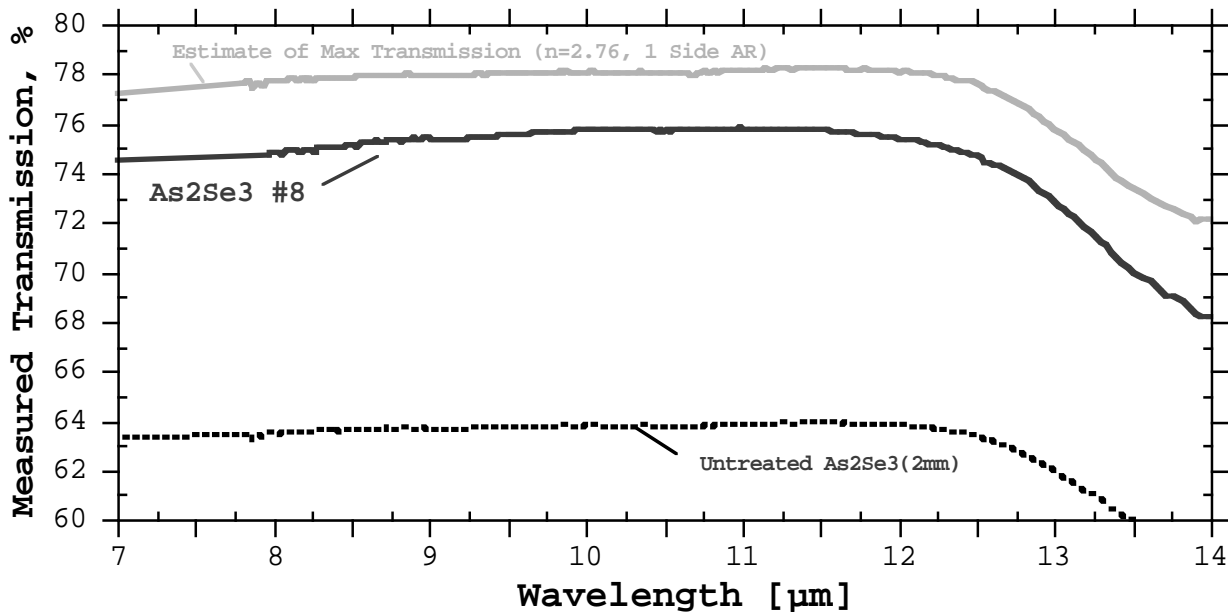


Figure 24: Measured transmission through an  $\text{As}_2\text{Se}_3$  window with a Motheye AR texture fabricated in one surface only.

#### 4. SUMMARY

AR surface relief microstructures have been shown to offer a significantly increased laser damage threshold for optics in high power laser systems over that attainable with conventional thin-film coatings. In addition, a new type of AR microtexture with a random distribution of surface structures has been shown to exhibit extremely broad-band performance. Random AR structures offer the potential for low cost fabrication through simplified processing requirements and through high volume replication techniques. The environmental durability of Random AR microstructures was investigated with promising initial results reported. Lastly, the potential for realizing AR microstructures in moldable infrared transmitting materials has been explored.

#### 5. ACKNOWLEDGEMENTS

Janos Technologies of New Hampshire supplied the samples of AMTIR4 for our internal Motheye development work, and provided FTIR measurements of our Random AR textures in glass. Omega Optical Inc. conducted the environmental testing and the resulting FTIR measurements. The work with silicon was supported by a 2006 Phase I SBIR sponsored by The Department of Defense, Missile Defense Agency, Wright Patterson Air Base. BAE systems of New Hampshire generously supplied ZGP crystals for use in the AR microstructure process development reported. This ZGP work was funded by a 2006 Phase I SBIR sponsored by The Department of Defense, Air Force Research Laboratory, Wright Patterson Air Base. All SEM analysis was performed by Mr. John Knowles at MicroVision Laboratories, Inc., (978-250-9909).

#### 6. REFERENCES

- [1] Hopkins, F. K., Fernelius, N. C., Goldstein, J. T., Zelmon, D. E., and Leininger, C. A., "Advances in nonlinear optical crystals", Proc. SPIE Vol. 5912, August 2005, pgs. 1-5.
- [2] Zawilski, K.T., Setzler, S. D., Schunemann, P.G., and Pollak, T. M. (BAE), "Laser damage threshold of single crystal ZnGeP<sub>2</sub> at 2.05  $\mu\text{m}$ ", Proc. of SPIE Vol. 5991, Dec. 2005
- [3] Krol, H., Gallais, L, Commandre, M., Grezes-Besset, C, Torricini, D., and Lagier, G., "LIDT improvement of multilayer coatings by accurate analysis of fabrication steps", Proc. of SPIE Vol. 5963, 2005
- [4] Kulakofsky, J., Lewis, W., Robertson, M., Moore, T., Krishnan, G., "Designing high-power components for optical telecommunications", Proc. of SPIE Vol. 4679, p. 198-210, April 2002.
- [5] C. J. Stolz, J. Adams, M. D. Shirk, M. A. Norton, T. L. Weiland, (LLNL) "Engineering meter-scale laser resistant coatings for the near IR", Proc. of SPIE Vol. 5963, Sept. 2005
- [6] M. R. Borden, J. A. Folta, C. J. Stolz, J. R. Taylor, J. E. Wolfe, A. J. Griffin, M. D. Thomas, (LLNL) "Improved method for laser damage testing coated optics", Proc. of SPIE Vol. 5991, Dec. 2005
- [7] Y. Bai, S. G. Bernd, J. R. Hosack, M. C. Farris, J. T. Montroy, J. Bajaj, (ROCKWELL) "Hybrid CMOS Focal Plane Array with Extended UV and NIR Response for Space Applications", Proc. of SPIE Vol. 5167, Jan. 2004
- [8] D. Macdonald, A. Cuevas, M. Kerr, C. Samundsett, D. Ruby, S. Winderbaum, and A. Leo, "Texturing Industrial Multicrystalline Silicon Solar Cells", ISES 2001 Solar World Congress.
- [9] Bernhard, C. G., "Structural and functional adaptation in a visual system", Endeavour, 26, pgs. 79-84, 1967
- [10] Clapham, P.B. and Hutley, M.C., "Reduction of lens reflexion by the 'Moth Eye' principle", Nature, 244, 281-2, Aug. 3, 1973)
- [11] Wilson, S.J. & Hutley, M.C., "The optical properties of 'moth eye' antireflection surfaces", Optica Acta, Vol. 29, No. 7, pgs 993-1009, 1982
- [12] Southwell, W. H., "Pyramid-array surface-relief structures producing antireflection index matching on optical surfaces", JOSA A, Vol. 8, No. 3, pgs 549-553, March 1991
- [13] Raguin, D.H. & Morris, G.M., "Antireflection structured surfaces for the infrared spectral region", Applied Optics, Vol. 32, No.7, pg 1154, March 1993
- [14] MacLeod, B.D., and Hobbs, D.S., "Low-Cost Anti-Reflection Technology For Automobile Displays", Journal of the Society for Information Display, Automotive Display Conference, November 2004.
- [15] D.S. Hobbs and B.D. MacLeod, "Design, Fabrication and Measured Performance of Anti-Reflecting Surface Textures in Infrared Transmitting Materials", Proc. SPIE Vol. 5786, May 2005.
- [16] Hobbs, D.S., et. al., "Automated Interference Lithography Systems for Generation of Sub-Micron Feature Size Patterns", SPIE Conference on Micromachine Technology for Diffractive and Holographic Optics, Proc. SPIE, Vol. 3879, September 1999, pg 124-136